A travelling wave approach to a multi-agent system with a path-graph topology

Dan Martinec[a], Ivo Herman[a,*], Michael Šebek[a]

[a] *Faculty of Electrical Engineering, Czech Technical University in Prague. Czech Republic*

arXiv:1410.0474v4 [cs.SY] 29 Mar 2016

Abstract

The paper presents a novel approach for the analysis and control of a multi-agent system with non-identical agents and a path-graph topology. With the help of irrational wave transfer functions, the approach describes the interaction among the agents from the 'local' perspective and identifies travelling waves in the system. It is shown that different dynamics of the agents creates a virtual boundary that causes a partial reflection of the travelling waves. Undesired effects due to the reflection of the waves, such as amplification/attenuation, long transients or string instability, can be compensated by the feedback controllers introduced in this paper. We show that the controllers achieve asymptotic and even string stability of the system.

Keywords: multi-agent system, travelling waves, wave transfer function, path graph, irrational transfer function

1. Introduction

A path graph is one of the simplest and most studied interaction topologies of a multi-agent system. In such a system each agent, except for the first and last one, interacts with its two neighbours. Despite its simplicity, a path-graph topology serves, for instance, as a model of vehicular platoons [25, 1], discretized flexible structures [21] or [4], or a spatially-discretized models of long electrical transmission lines [3].

A distributed system defined over a path graph is most often analyzed using state-space techniques and algebraic graph theory. For instance, stability and convergence rate of the system depend on the eigenvalues of the Laplacian matrix [19]. Scaling of $\mathcal{H}_2$ and $\mathcal{H}_\infty$ norms of a path-graph system was investigated in [7, 11]. The effect of disturbance was investigated in [8] using port-Hamiltonian approach. A good scaling can be captured by a term string stability. Roughly speaking, in a string-stable system a disturbance is not amplified as it propagates among agents (for vehicular platoons [5], for general systems [24]). However, often the results in the literature rely on the assumption of identical agents. Moreover, they give overall behavior of the system, so it is hard to infer from them what happens in the middle of the platoon or near the boundaries.

Following the ideas of other researchers (e.g., [1, 6]), we will describe the system using wave perspective. Indeed, the propagation of the change in the multi-agent system can be described with the help of travelling waves. We will illustrate it on an example of a system with identical agents and a path-graph topology. If the first agent changes its output, then all following agents sequentially respond to this change. If we study their response from the local point of view [16, 13, 22] we can notice that the change is propagated as a wave. The wave departs from the first agent and travels along the system to the last agent, where it reflects and travels back. When it reaches the first agent, it reflects again. The same phenomenon is apparent if the agents are non-identical—the travelling wave is partially reflected on non-identical agents [14]. We can imagine this behaviour as the reflection of the wave if it encounters a boundary between two media of different properties.

The tool for analysis will be so called *wave transfer function* (WTF). The transfer-function approach to waves has recently been revisited in a series of papers for lumped models (see [16, 26]) and for continuous flexible structures [22]. The travelling wave approach has also been applied to vibration control [15] and it seems to be related to the impedance matching in the power networks [10]. The wave-based description leads to irrational transfer functions, analysis of which differs in several aspects from their rational counterparts [2].

This paper continues in the research started in [13], where waves in a platoon of identical vehicles is considered. A natural extension of this model is to consider a chain of non-identical (heterogeneous) agents. The first step in the treatment of non-identical agents using travelling waves is given in [17] for a mass-spring model. We generalize it by considering an arbitrary dynamics of the agents and their controllers. The preliminary results are presented in [14], where we introduced the *soft boundary* in a chain of vehicles. Here, we follow this concept of boundaries in a multi-agent system and introduce the second fundamental type of boundary, the *hard boundary*. Although the boundaries are virtual in nature, they principally affect the overall system behaviour. We present some fundamental properties of the boundaries and design wave-absorbing controllers for both types of boundaries.

The main contributions of the paper are: i) mathematical description of the travelling waves in a multi-agent system with non-identical agents given by Theorems 1 and 2, ii) a design

☆The research was supported by the Czech Science Foundation within the project GACR 16-19526S.

*Corresponding author

Email addresses: dan.martinec@fel.cvut.cz (Dan Martinec), ivo.herman@fel.cvut.cz (Ivo Herman), sebekm1@fel.cvut.cz (Michael Šebek)

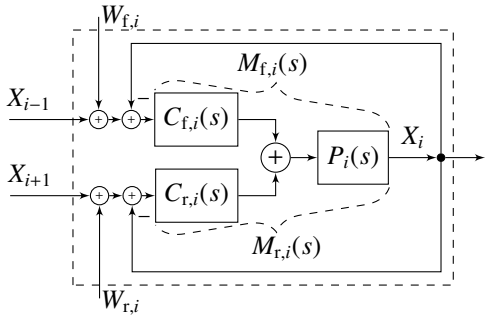

Figure 1: The model of ith agent.

of a controller that prevents a reflection of the travelling wave (Theorems 3 and 4) and iii) proof of stability and string stability when these controllers are used (Theorem 5). For better understanding and easy simulations, we provide a set of functions in MATLAB, see *WaveBox* [12].

2. System model

We consider a multi-agent system of N non-identical agents with a path-graph interaction topology, for instance, a platoon of vehicles on a highway. In this case the goal of the system is to drive along a line with equal distances between the agents.

The dynamics of agents is described by a linear single-input-single-output model with the transfer function $P_i(s)$, where i is the index of the agent. The output, $X_i(s)$, is given as $X_i(s) = P_i(s)U_i(s)$, where $U_i(s)$ is the input to the agent model generated by a control law. This control law is the local relative output feedback between the agent i and its two neighbouring agents $i-1$ and $i+1$. It is modelled as

$$\begin{aligned} U_i(s) =& C_{\mathrm{f},i}(s)(X_{i-1}(s) - X_i(s)) + C_{\mathrm{r},i}(s)(X_{i+1}(s) - X_i(s)) \\ &+ C_{\mathrm{f},i}(s)W_{\mathrm{f},i}(s) + C_{\mathrm{r},i}(s)W_{\mathrm{r},i}(s), \end{aligned} \tag{1}$$

where $C_{\mathrm{f},i}(s)$ is the transfer function of the controller for the front output difference $X_{i-1}(s) - X_i(s)$ and $C_{\mathrm{r},i}(s)$ is the transfer function of the rear controller. $W_{\mathrm{f},i}(s)$ and $W_{\mathrm{r},i}(s)$ are additional inputs to the agent. We assume that the inputs are equal to zero unless we specify them otherwise. Since in the whole paper we work with transfer functions. we will often omit the argument '(s)' when no ambiguity seems possible. Denote the front open-loop transfer function (OLTF) and rear OLTF by $M_{\mathrm{f},i}(s) = P_i(s)C_{\mathrm{f},i}(s)$ and $M_{\mathrm{r},i}(s) = P_n(s)C_{\mathrm{r},i}(s)$, respectively. The model of the ith agent with zero initial conditions then is

$$\begin{aligned} X_i(s) =& M_{\mathrm{f},i}(s)(X_{i-1}(s) - X_i(s)) + M_{\mathrm{r},i}(s)(X_{i+1}(s) - X_i(s)) \\ &+ M_{\mathrm{f},i}(s)W_{\mathrm{f},i}(s) + M_{\mathrm{r},i}(s)W_{\mathrm{r},i}(s). \end{aligned} \tag{2}$$

It is depicted in Fig. 1. Usually, there is at least one integrator both in the front and rear OLTFs (for instance, from velocity to position), such that the OLTF can be factored as $M(s) = 1/s^{\nu}\overline{M}(s)$, where $\overline{M}(0) < \infty$ and ν is the number of integrators in the corresponding open loop (either $M_{\mathrm{f},i}$ or $M_{\mathrm{r},i}$).

The first agent is described as $X_1(s) = M_{\mathrm{f},1}(s)(W_{\mathrm{f},1}(s) - X_1(s)) + M_{\mathrm{r},1}(s)(X_2(s) - X_1(s))$, where $W_{\mathrm{f},1}(s) = X_{\mathrm{ref}}(s)$ is the external input, which represents the reference for the system (for instance, a virtual leader). This is the input from which the system is to be controlled. The last agent $i = N$ is controlled as $X_N(s) = M_{\mathrm{f},N}(s)(X_{N-1}(s) - X_N(s))$.

2.1. Wave transfer function

The key idea of the wave approach is that the output of the ith agent is decomposed into two components, $A_i(s)$ and $B_i(s)$ such that $X_i(s) = A_i(s) + B_i(s)$. The component $A_i(s)$ represents a wave which propagates in the forward direction, that is, to the agents with higher indices. The component $B_i(s)$ represents the wave in the backward direction—to the agents with lower indices. The idea is similar to the standard D'Alambert solution of the wave equation in PDE, where also two waves propagating in different directions appear.

Now we summarize the results of [13], where we considered identical agents. In this case $M_{\mathrm{f},i}(s) = M_{\mathrm{r},i}(s) = M(s)$. The *Wave transfer function* $G(s)$ (abbreviated as WTF) captures how the wave propagates in the system in one direction, that is $A_{i+1}(s) = G(s)A_i(s)$ and $B_{i-1}(s) = G(s)B_i(s)$. There is a simple way how to derive this transfer function. Consider a path graph with infinite number of agents and with only a wave propagating in the forward direction. The wave will never reflect back, so $X_n(s) = A_n(s)$. Then WTF is given by $G(s) = X_{i+1}(s)/X_i(s)$ for $N \to \infty$, see [13, Sec. 3.1]. When $W_{\mathrm{f},i} = W_{\mathrm{r},i} = 0$, the system with identical agents is described for $i \in [1, N-1]$ as [13]

$$X_i(s) = A_i(s) + B_i(s), \tag{3}$$

$$A_{i+1}(s) = G(s)A_i(s), \tag{4}$$

$$B_i(s) = G(s)B_{i+1}(s), \tag{5}$$

$$G(s) = \frac{1}{2}\alpha(s) - \frac{1}{2}\sqrt{\alpha^2(s) - 4}, \tag{6}$$

where $\alpha(s) = 2 + 1/M(s)$, or, alternatively, $\alpha(s) = G(s) + G^{-1}(s)$. The function $G^{-1}(s) = 1/G(s) = \frac{1}{2}\alpha(s) + \frac{1}{2}\sqrt{\alpha^2(s) - 4}$. We now explain the traveling wave concept. Combining (3)-(5),

$$X_i(s) = G(s)A_{i-1}(s) + G(s)B_{i+1}(s). \tag{7}$$

This means that the wave $A_{i-1}(s)$ coming from the left is transformed through the transfer function $G(s)$ and summed with the transformed wave from the right $G(s)B_{i+1}(s)$.

There are only two boundaries in the homogeneous system. The *forced-end boundary*, located at the first agent, is given by

$$A_1(s) = G(s)W_{\mathrm{f},1}(s) - G^2(s)B_1(s). \tag{8}$$

and the *free-end boundary*, located at the rear-end agent, is

$$B_N(s) = G(s)A_N(s). \tag{9}$$

The first case is analogous to Dirichlet boundary condition and the second to Neumann. The system with boundaries is shown in Fig. 2. For both types of the boundaries, a wave-absorbing controller can be designed to prevent a reflection of the incident wave. The controller absorbs the travelling wave by calculating the incident part of the wave and adding this part to its output. With the controller, the input to the first agent changes to

$$W_{\mathrm{f},1}(s) = X_{\mathrm{ref}}(s) + G(s)B_1(s) = G(s)X_1(s) + (1 - G(s)^2)X_{\mathrm{ref}}(s). \tag{10}$$

Such absorber can qualitatively improve the transient. This concludes the brief summary of [13].

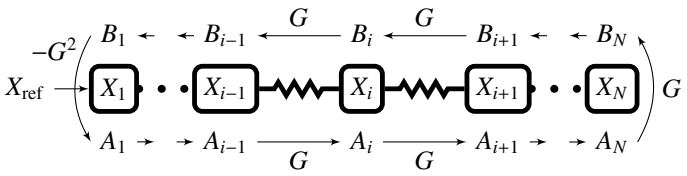

Figure 2: Scheme of a multi-agent system with identical agents. The squares are agents with local dynamics described by (2). The virtual connections, created by the local control law, are illustrated by springs.

2.2. *Soft and hard boundaries*

Now let us go back to the heterogeneous system of non-identical agents. There are additional boundaries between the agents having different models. In general, we can distinguish between three cases: i) $M_{\mathrm{r},i}(s) \neq M_{\mathrm{f},i+1}(s)$, ii) $M_{\mathrm{f},i}(s) \neq M_{\mathrm{r},i}(s)$, and iii) a combination of i) and ii). As we will see, they cause a partial reflection of the travelling wave. In order to derive its mathematical properties, we assume that the boundary of interest is the only boundary in the system. This also means that all the agents to left of the boundary are identical. Let the WTF for the agents to the left be $G(s)$. Similarly, the agents to the right of the boundary are identical and the WTF for them is $H(s)$.

We will focus on the boundaries caused by i) and ii). Once their properties are known, the description of their combination iii) is easy. Thus, we do not discuss it in this paper.

Definition 1. *Soft boundary* is a virtual boundary between two agents, indexed σ and $\sigma+1$, with the property $M_{\mathrm{r},\sigma}(s) \neq M_{\mathrm{f},\sigma+1}(s)$.

The soft boundary is, for instance, located in a platoon of non-identical vehicles governed by the same symmetric bidirectional control law or in a mass-spring model with identical springs but non-identical masses. The wave transfer function between the agents with index $i \leq \sigma$ is $G(s)$ and between the agents with $i \geq \sigma+1$ it is $H(s)$, given as

$$G(s) = \frac{1}{2}\alpha_1 - \frac{1}{2}\sqrt{\alpha_1^2 - 4}, \quad H(s) = \frac{1}{2}\alpha_2 - \sqrt{\alpha_2^2 - 4}, \tag{11}$$

where $\alpha_1 = 2 + 1/M_{\mathrm{r},\sigma}(s)$ and $\alpha_2 = 2 + 1/M_{\mathrm{f},\sigma+1}(s)$. For the agents with indices $i \leq \sigma$ holds $M_{\mathrm{f},i} = M_{\mathrm{r},i} = M_{\mathrm{r},\sigma}$ and for agents $i \geq \sigma+1$ holds $M_{\mathrm{f},i} = M_{\mathrm{r},i} = M_{\mathrm{f},\sigma+1}$. The irrational transfer functions were obtained identically as in [13, Sec. 3.1].

The second type of boundary is defined as follows.

Definition 2. The *hard boundary* is a virtual boundary located at the ηth agent with the property $M_{\mathrm{f},\eta}(s) \neq M_{\mathrm{r},\eta}(s)$.

The hard boundary is, for instance, located in a platoon of identical vehicles with asymmetric control, see [1], or in a mass-spring model with identical masses but different springs.

The adjective 'hard' emphasizes the fact that the boundary is located at an agent, in contrast to the soft boundary, located between two agents. To distinguish between the incident, transmitted and reflected waves at the hard boundary, we decompose

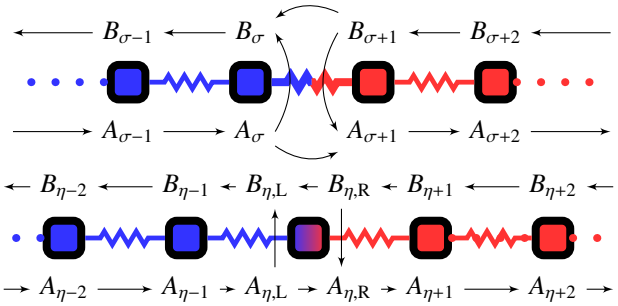

Figure 3: A system with the soft (top) and hard (bottom) boundary. The blue and red squares are agents with the WTFs $G(s)$ and $H(s)$ in (11), (15). The blue-red spring is the soft boundary and the blue-red square is the hard boundary.

X_η to the hard-boundary wave components as

$$X_\eta(s) = A_{\eta,\mathrm{L}}(s) + B_{\eta,\mathrm{L}}(s) = A_{\eta,\mathrm{R}}(s) + B_{\eta,\mathrm{R}}(s), \tag{12}$$

where the indexes L and R denote the wave components that are next to the left and right sides of the boundary, respectively. They are tied by the following.

$$A_{\eta,\mathrm{L}}(s) = G(s)A_{\eta-1}(s), \quad B_{\eta,\mathrm{L}}(s) = G^{-1}(s)B_{\eta-1}(s), \tag{13}$$

$$A_{\eta,\mathrm{R}}(s) = H^{-1}(s)A_{\eta+1}(s), \quad B_{\eta,\mathrm{R}}(s) = H(s)B_{\eta+1}(s), \tag{14}$$

where WTFs to the left and right of the boundary are

$$G(s) = \frac{1}{2}\alpha_1 - \frac{1}{2}\sqrt{\alpha_1^2 - 4}, \quad H(s) = \frac{1}{2}\alpha_2 - \sqrt{\alpha_2^2 - 4}, \tag{15}$$

and $\alpha_1 = 2 + 1/M_{\mathrm{f},\eta}(s)$ and $\alpha_2 = 2 + 1/M_{\mathrm{r},\eta}(s)$. Both boundaries are illustrated in Fig. 3.

3. Mathematical description of waves in path graph

In this section we will concentrate on the description of the boundaries and their effect on the propagating wave.

Theorem 1 ([14])**.** *Let $G(s)$ and $H(s)$ be given by (11). Then a soft boundary is in the Laplace domain described by four boundary-transfer functions (BTFs)*

$$T_{\mathrm{aa}} = \frac{A_{\sigma+1}}{A_\sigma} = \frac{H - HG^2}{1 - HG}, \quad T_{\mathrm{ba}} = \frac{A_{\sigma+1}}{B_{\sigma+1}} = \frac{HG - H^2}{1 - HG}, \tag{16}$$

$$T_{\mathrm{bb}} = \frac{B_\sigma}{B_{\sigma+1}} = \frac{G - H^2G}{1 - HG}, \quad T_{\mathrm{ab}} = \frac{B_\sigma}{A_\sigma} = \frac{HG - G^2}{1 - HG}, \tag{17}$$

The proof is given in [14]. The interpretation is that if there is a wave travelling to the soft boundary from the left-hand side, then it is partially reflected from the boundary (described by T_{ab}) and partially transmitted through the boundary (by T_{aa}). Likewise, if the wave travels from the opposite side, then the transfer functions T_{ba} and T_{bb} represent the respective waves. When combined,

$$X_\sigma(s) = G(s)(1 + T_{\mathrm{ab}}(s))A_{\sigma-1}(s) + T_{\mathrm{bb}}(s)B_{\sigma+1}(s), \tag{18}$$

$$X_{\sigma+1}(s) = H(s)(1 + T_{\mathrm{ba}}(s))B_{\sigma+2}(s) + T_{\mathrm{aa}}(s)A_\sigma(s). \tag{19}$$

The forced-end boundary is an example of the soft boundary. Substituting $G = 0$ into (16) and (17) gives $T_{\rm aa} = H$, $T_{\rm ba} = -H^2$ and $T_{\rm bb} = T_{\rm ab} = 0$. In addition, if $G(s) = H(s)$ (there is no boundary), there there is no reflection ($T_{\rm ab}(s) = T_{\rm ba}(s) = 0$) and everything gets through ($T_{\rm aa}(s) = G(s), T_{\rm bb}(s) = G(s)$).

Theorem 2. *Let G and H be given by (15). Then the BTFs describing the hard boundary in the Laplace domain are*

$$T_{\rm AA} = \frac{A_{\eta,\rm R}}{A_{\eta,\rm L}} = \frac{(1+G)(1-H)}{1-HG}, \quad T_{\rm BA} = \frac{A_{\eta,\rm R}}{B_{\eta,\rm R}} = \frac{H-G}{1-HG}, \tag{20}$$

$$T_{\rm BB} = \frac{B_{\eta,\rm L}}{B_{\eta,\rm R}} = \frac{(1+H)(1-G)}{1-HG}, \quad T_{\rm AB} = \frac{B_{\eta,\rm L}}{A_{\eta,\rm L}} = \frac{G-H}{1-HG}, \tag{21}$$

Proof. From (2), the output of the agent can be rewritten as

$$X_\eta(s) = T_{\rm L}(s)X_{\eta-1}(s) + T_{\rm R}(s)X_{\eta+1}(s), \tag{22}$$

where $T_{\rm L} = M_{{\rm f},\eta}/(1 + M_{{\rm f},\eta} + M_{{\rm r},\eta})$ and $T_{\rm R} = M_{{\rm r},\eta}/(1 + M_{{\rm f},\eta} + M_{{\rm r},\eta})$. We combine (3), (13) and (14) to obtain $X_{\eta-1} = A_{\eta-1} + B_{\eta-1} = G^{-1}A_{\eta,\rm L} + GB_{\eta,\rm L}$ and $X_{\eta+1} = A_{\eta+1} + B_{\eta+1} = HA_{\eta,\rm R} + H^{-1}B_{\eta,\rm R}$. Substituting these equations into (22) and using (12) for X_η yields

$$A_{\eta,\rm L}(1-T_{\rm L}G^{-1}) + B_{\eta,\rm L}(1-T_{\rm L}G) = B_{\eta,\rm R}(T_{\rm R}H^{-1}) + A_{\eta,\rm R}T_{\rm R}H. \tag{23}$$

The four wave components are now reduced to three components by substituting $A_{\eta,\rm R} = A_{\eta,\rm L} + B_{\eta,\rm L} - B_{\eta,\rm R}$ or by $B_{\eta,\rm L} = A_{\eta,\rm R} + B_{\eta,\rm R} - A_{\eta,\rm L}$ into (23). These substitutions give

$$B_{\eta,\rm L} = B_{\eta,\rm R}\frac{T_{\rm R}H - T_{\rm R}H^{-1}}{T_{\rm L}G + T_{\rm R}H - 1} + A_{\eta,\rm L}\frac{1 - T_{\rm L}G^{-1} - T_{\rm R}H}{T_{\rm L}G + T_{\rm R}H - 1}, \tag{24}$$

$$A_{\eta,\rm R} = A_{\eta,\rm L}\frac{T_{\rm L}G - T_{\rm L}G^{-1}}{T_{\rm L}G + T_{\rm R}H - 1} + B_{\eta,\rm R}\frac{1 - T_{\rm L}G - T_{\rm R}H^{-1}}{T_{\rm L}G + T_{\rm R}H - 1}. \tag{25}$$

These formulas can be further simplified by expressing $T_{\rm L}$ and $T_{\rm R}$ in terms of G and H. Specifically, $M_{{\rm f},\eta} = (G + G^{-1} - 2)^{-1}$ and $M_{{\rm r},\eta} = (H + H^{-1} - 2)^{-1}$. Substituting for them into (24) and (25) yields the result. □

The theorem states that wave incident from the left side of the hard boundary (described by $A_{\eta,\rm L}$) is partially reflected from the boundary (described by $T_{\rm AB}$) and partially transmitted through the boundary (by $T_{\rm AA}$). For the wave incident to the opposite side (described by $B_{\eta,\rm R}$), the transfer functions are $T_{\rm BA}$ and $T_{\rm BB}$, respectively. The output of the hard-boundary agent can be expressed in two equivalent ways,

$$X_\eta = G(1 + T_{\rm AB})A_{\eta-1} + HT_{\rm BB}B_{\eta+1}, \tag{26}$$

$$X_\eta = GT_{\rm AA}A_{\eta-1} + H(1 + T_{\rm BA})B_{\eta+1}. \tag{27}$$

The free-end boundary from (9) is an example of the hard boundary. In this case $H = 0$, which gives $T_{\rm AA} = T_{\rm BB} = G$ and $T_{\rm AB} = T_{\rm BA} = 0$. Again, if $G(s) = H(s)$, then $T_{AB} = T_{BA} = 0$ and $T_{AA} = T_{BB} = 1$ which converts (26), (27) into (3).

3.1. Properties of the boundaries

Although the above descriptions of the boundaries are different, they have some common features. The following result is a direct application of Theorems 1 and 2.

Corollary 1. *The soft and hard BTFs are related as follows,*

$$T_{\rm aa}(s) = T_{\rm BB}(s) + G(s) - 1, \quad T_{\rm ba}(s) = H(s)T_{\rm AB}(s), \tag{28}$$

$$T_{\rm bb}(s) = T_{\rm AA}(s) + H(s) - 1, \quad T_{\rm ab}(s) = G(s)T_{\rm BA}(s), \tag{29}$$

$$T_{\rm AA}(s) = 1 + T_{\rm AB}(s), \quad T_{\rm BB}(s) = 1 + T_{\rm BA}(s), \tag{30}$$

$$T_{\rm AA}(s) + T_{\rm BB}(s) = 2, \quad T_{\rm AB}(s) + T_{\rm BA}(s) = 0. \tag{31}$$

We define the DC gain $\kappa_{\rm G}$ of $G(s)$ as $\kappa_{\rm G} = \lim_{s\to 0} G(s)$. Recall that ν is the number of integrators in the open loop.

Corollary 2. *Let $\kappa_{\rm aa}$ be the DC gain of $T_{\rm aa}$, $\kappa_{\rm ab}$ be the DC gain of $T_{\rm ab}$ etc. If $\nu \geq 1$ for both front and rear OLTFs, then*

$$\kappa_{\rm aa} + \kappa_{\rm bb} = 2, \quad \kappa_{\rm ab} + \kappa_{\rm ba} = 0, \tag{32}$$

$$\kappa_{\rm aa} - \kappa_{\rm ab} = 1, \quad \kappa_{\rm bb} - \kappa_{\rm ba} = 1, \tag{33}$$

$$\kappa_{\rm aa} = \kappa_{\rm BB}, \quad \kappa_{\rm ba} = \kappa_{\rm AB}, \quad \kappa_{\rm bb} = \kappa_{\rm AA}, \quad \kappa_{\rm ab} = \kappa_{\rm BA}, \tag{34}$$

Proof. Under the above assumptions, the DC gain of a WTF is one, i.e. $\lim G(s)_{s\to 0} = 1$ and $\lim H(s)_{s\to 0} = 1$ [13]. Then, the proof is a straightforward application of Corollary 1. □

The DC gains of WTFs and BTFs can be used to approximate the value of the transient (see Sec. 5.2). The following values of $\kappa_{\rm aa}$ and $\kappa_{\rm bb}$ are proved in Appendix A.

Lemma 1. *Let $\nu_{\rm r}, \nu_{\rm f}$ be the number of integrators in $M_{{\rm r},\sigma}$ and $M_{{\rm f},\sigma+1}$, respectively. Assume that $\nu_{\rm f} \geq 1, \nu_{\rm r} \geq 1$. Then we get the DC gains of the soft boundary as*

$$\kappa_{\rm aa} = 2\left(\sqrt{\frac{n_{1,0}d_{2,0}}{n_{2,0}d_{1,0}}} + 1\right)^{-1}, \ \kappa_{\rm bb} = 2\left(\sqrt{\frac{n_{2,0}d_{1,0}}{n_{1,0}d_{2,0}}} + 1\right)^{-1}, \tag{35}$$

for $\nu_{\rm f} = \nu_{\rm r}$, $\kappa_{\rm aa} = 0, \kappa_{\rm bb} = 2$ for $\nu_{\rm f} < \nu_{\rm r}$, and $\kappa_{\rm aa} = 2, \kappa_{\rm bb} = 0$ for $\nu_{\rm f} > \nu_{\rm r}$. The constants are $n_{1,0}/d_{1,0} = \lim_{s\to 0} s^{\nu_{\rm r}} M_{{\rm r},\sigma}$, $n_{2,0}/d_{2,0} = \lim_{s\to 0} s^{\nu_{\rm f}} M_{{\rm f},\sigma+1}$.

Corollary 3. *If $\nu \geq 1$ both in front OLTF and rear OLTF, then the DC gains are bounded as*

$$-1 \leq \kappa_{\rm ab}, \kappa_{\rm ba}, \kappa_{\rm AB}, \kappa_{\rm BA} \leq 1, \tag{36}$$

$$0 \leq \kappa_{\rm aa}, \kappa_{\rm bb}, \kappa_{\rm AA}, \kappa_{\rm BB} \leq 2. \tag{37}$$

Proof. The soft-boundary DC gains come from Lemma 1 and Corollary 2, the hard-boundary DC gains from Corollary 2. □

4. Controllers for the boundaries

We now design a feedback controller compensating the fact that the agents are not identical. The motivation is to prevent the undesired reflection of the wave to shorten the settling time. To control the wave at the boundary, we first have to assume that the input in (2) is nonzero and investigate its properties. For now, we consider only the input $W_{{\rm r},i}$ and we set $W_{{\rm f},i} = 0$. Hence, the model (2) of the nth agent changes to

$$X_i(s) = M_{{\rm f},i}(s)(X_{i-1}(s) - X_i(s)) + M_{{\rm r},i}(s)(X_{i+1}(s) - X_i(s) + W_{{\rm r},i}(s)). \tag{38}$$

The input $W_{\mathrm{r},i}(s)$ generates a wave that propagates in the system in the same manner as (4) and (5), only (7) is changed as follows

$$X_i(s) = G(s)A_{i-1}(s) + G(s)B_{i+1}(s) + T_{\mathrm{r},i}(s)W_{\mathrm{r},i}(s), \tag{39}$$

where $T_{\mathrm{r},i}(s) = X_i(s)/W_{\mathrm{r},i}(s)$ for $N \to \infty$. We are interested in finding $T_{\mathrm{r},i}(s)$, hence, we substitute (4)-(5) into (38) and get

$$T_{\mathrm{r},i}(s) = \frac{M_{\mathrm{r},i}(s)}{1 + (1 - G(s))M_{\mathrm{f},i}(s) + (1 - G(s))M_{\mathrm{r},i}(s)}. \tag{40}$$

Analogously, we can calculate the transfer function $T_{\mathrm{f},i}(s) = X_i(s)/W_{\mathrm{f},i}$ for a non-zero input $W_{\mathrm{f},i}$.

4.1. The soft boundary controller

A soft-boundary controller can be designed for various purposes, for instance, to prevent or modify a wave's transmission through the boundary. We now design an absorbing controller that prevents the reflection of a wave from the left side of the soft boundary. The derivation for its right side is analogous.

Suppose that the soft boundary is between agents σ and $\sigma+1$. By the combination of (18) and (40), we get

$$X_\sigma = (1 + T_{\mathrm{ab}})A_\sigma + T_{\mathrm{bb}}B_{\sigma+1} + T_{\mathrm{r},i}(1 + T_{\mathrm{ab}})W_{\mathrm{r},\sigma}. \tag{41}$$

The reflection of the wave travelling from the left is described by the term $T_{\mathrm{ab}}A_\sigma$. Therefore, we set $W_{\mathrm{r},\sigma}(s) = F_{\mathrm{f,S}}(s)A_\sigma(s)$, where $F_{\mathrm{f,S}}(s)$ is a transfer function of a controller to be found. To prevent the reflection, we eliminate the term $T_{\mathrm{ab}}A_\sigma$ by requiring $T_{\mathrm{ab}}(s)A_\sigma(s) + T_{\mathrm{r},i}(s)(1 + T_{\mathrm{ab}}(s))F_{\mathrm{f,S}}(s)A_\sigma(s) = 0$, from which we calculate the controller,

$$F_{\mathrm{f,S}}(s) = \frac{-T_{\mathrm{ab}}(s)}{T_{\mathrm{r},i}(s)(1 + T_{\mathrm{ab}}(s))}. \tag{42}$$

Substituting for $T_{\mathrm{ab}}(s)$ from (17) and for $T_{\mathrm{r},i}(s)$ from (40), the controller simplifies to $F_{\mathrm{f,S}}(s) = G(s) - H(s)$.

It remains to specify A_σ, which represents a wave incident to the soft boundary from the left. By (3)-(7), we have $A_\sigma(s) = G(X_{\sigma-1} - B_{\sigma-1}) = GX_{\sigma-1} - G^2(X_\sigma - A_\sigma)$, so we can write

$$A_\sigma(s) = \frac{G(s)}{1 - G^2(s)}X_{\sigma-1}(s) - \frac{G^2(s)}{1 - G^2(s)}X_\sigma(s). \tag{43}$$

Therefore, we have everything for the left-side absorbing control law $C_{\mathrm{L,S}} = M_{\mathrm{r},\sigma}F_{\mathrm{f,S}}A_\sigma$. Similarly, we can calculate the right-side absorbing control $C_{\mathrm{R,S}} = M_{\mathrm{r},\sigma}F_{\mathrm{r,S}}A_\sigma$. They are:

$$C_{\mathrm{L,S}} = M_{\mathrm{r},\sigma}\frac{G\,(G - H)}{1 - G^2}\,(X_{\sigma-1} - GX_\sigma)\,. \tag{44}$$

$$C_{\mathrm{R},S} = M_{\mathrm{f},\sigma+1}\frac{H(H - G)}{1 - H^2}\,(X_{\sigma+1} - HX_\sigma)\,. \tag{45}$$

Theorem 3. *The control law preventing any wave to be reflected from the soft boundary in the Laplace domain is*

$$X_\sigma = M_{\mathrm{r},\sigma}(X_{\sigma-1} - 2X_\sigma + X_{\sigma+1}) + C_{\mathrm{L},S}\,, \tag{46}$$

$$X_{\sigma+1} = M_{\mathrm{f},\sigma+1}(X_\sigma - 2X_{\sigma+1} + X_{\sigma+2}) + C_{\mathrm{R},S}\,, \tag{47}$$

where $C_{\mathrm{L},S}, C_{\mathrm{R},S}$ are given in (44), (45).

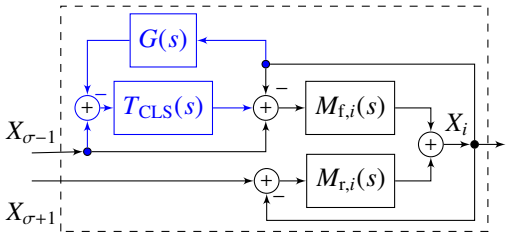

Figure 4: The model of σth agent with the left-side absorbing controller (blue), where $T_{\mathrm{CLS}} = G(s)(G(s) - H(s))/(1 - G^2(s))$ from (44).

The σth agent with implemented left-side absorbing controller is shown in Fig. 4. We calculate the wave propagation with the with the left- and right-side absorber implemented. By modifying (41), the outputs of the agents σ, $\sigma + 1$ are

$$\begin{aligned} X_\sigma =&(1 + T_{\mathrm{ab}})A_\sigma + T_{\mathrm{bb}}B_{\sigma+1} + F_{\mathrm{f,S}}T_{\mathrm{r},i}(1 + T_{\mathrm{ab}})A_\sigma \\ &+ T_{\mathrm{bb}}F_{\mathrm{r,S}}T_{\mathrm{f},i}B_{\sigma+1} = GA_{\sigma-1} + GB_{\sigma+1}, \end{aligned} \tag{48}$$

$$X_{\sigma+1} = HA_\sigma + HB_{\sigma+2}. \tag{49}$$

Both correspond to a wave propagation in homogeneous system (7). Theorem 3 describes the only control law that fully absorbs the wave ($T_{\mathrm{ab}}A_\sigma$ in (41) was cancelled by the unique $W_{\mathrm{r},\sigma}$).

4.2. The hard boundary controller

Controlling the hard boundary is similar to that of the soft boundary. Here, we only provide a brief description of the absorbing-controller design. The output of the ηth agent from (26) controlled with additional input $W_{\mathrm{f},\eta}(s)$ is

$$X_\eta = (1 + T_{\mathrm{AB}})A_{\eta,\mathrm{L}} + T_{\mathrm{BB}}B_{\eta,\mathrm{R}} + T_{\mathrm{f},i}W_{\mathrm{f},\eta}, \tag{50}$$

where $W_{\mathrm{f},\eta}(s) = F_{\mathrm{f,H}}(s)A_{\eta,\mathrm{L}}(s)$ and $F_{\mathrm{f,H}}(s)$ is a transfer function of a controller that prevents the reflection of a wave. To prevent the reflection of the wave travelling towards the hard boundary from the left, we set $T_{\mathrm{AB}}A_{\eta,\mathrm{L}} = -F_{\mathrm{f,H}}T_{\mathrm{f},i}W_{\mathrm{f},\eta}$. Hence,

$$F_{\mathrm{f,H}}(s) = -\frac{T_{\mathrm{AB}}(s)}{T_{\mathrm{f},i}(s)} = \frac{(H(s) - G(s))(1 - G(s))}{G(s)(1 - H(s))}. \tag{51}$$

The $A_{\eta,\mathrm{L}}$ term represents the wave travelling towards the hard boundary from left, which is again computed by (43),

$$A_{\eta,\mathrm{L}}(s) = \frac{G(s)}{1 - G^2(s)}X_{\eta-1}(s) - \frac{G^2(s)}{1 - G^2(s)}X_\eta(s). \tag{52}$$

The left-side and right-side (calculated similarly) absorbing control laws are then

$$C_{\mathrm{L,H}} = M_{\mathrm{f},\eta}F_{\mathrm{f,H}}A_{\eta,\mathrm{L}} = M_{\mathrm{f},\eta}\frac{H - G}{(1+G)(1-H)}(X_{\eta-1} - GX_\eta), \tag{53}$$

$$C_{\mathrm{R,H}} = M_{\mathrm{r},\eta}F_{\mathrm{r,H}}A_{\eta,\mathrm{R}} = M_{\mathrm{r},\eta}\frac{G - H}{(1+H)(1-G)}(X_{\eta+1} - HX_\eta). \tag{54}$$

Theorem 4. *The control law that prevents any wave to be reflected from the hard boundary in the Laplace domain is*

$$X_\eta = M_{\mathrm{f},\eta}(X_{\eta-1} + X_\eta) + M_{\mathrm{r},\eta}(X_{\eta+1} - X_\eta) + C_{\mathrm{L,H}} + C_{\mathrm{R,H}}, \tag{55}$$

where $C_{\mathrm{L,H}}, C_{\mathrm{R,H}}$ are given in (53), (54).

The control laws implemented on the agent η using (30) give

$$X_\eta(s) = A_{\eta,\mathrm{L}}(s) + B_{\eta,\mathrm{R}}(s) = G(s)A_{\eta-1}(s) + H(s)B_{\eta+1}(s), \quad (56)$$

Combining (56) and (12) gives $A_{\eta,\mathrm{L}} = A_{\eta,\mathrm{R}}$ and $B_{\eta,\mathrm{L}} = B_{\eta,\mathrm{R}}$. In words, the hard boundary between the wave components indexed by L and R is removed at the ηth agent and the wave transmits through the agent without being reflected. By comparison of Theorems 3 and 4 we can see that we need to implement the wave absorber on two agents for the soft boundary but only on one agent for the hard boundary.

4.3. Stability of the controllers

To prove stability of the control law, we first need to prove stability of the WTF. The proof is given in Appendix B.

Lemma 2. *If $M(s)$ is proper and has no CRHP (closed right half-plane) zeros and no CRHP poles, except for poles at the origin, and if $1 + 4M(\jmath\omega)$ does not intersect the non-positive real axis for $\omega \in (0, \infty)$, then the wave transfer function $G(s)$ corresponding to $M(s)$ is asymptotically stable.*

We show below that the controllers do not destabilize the system (proof is in Appendix C). The opposite is true: their use make the system even string stable for arbitrary platoon size. This guarantees very good transients.

Definition 3 ([5]). A system is called L_2 string stable if there is an upper bound on the L_2-induced system norm of $T_{0,i}(s)$ that does not depend on the number of agents, where $T_{0,i}(s) = \frac{X_i(s)}{X_{\mathrm{ref}}(s)}$.

Theorem 5. *If the WTFs are asymptotically stable, then the multi-agent system with the path-graph topology and the control law from Theorem 3 or Theorem 4 is asymptotically stable. Furthermore, these control laws implemented with the wave absorber, located on the first or rear-end agent, make the multi-agent system L_2 string stable.*

4.4. Discussion of wave controllers

The advantage of the wave controller is that it allows the modification of the reflection conditions for the travelling waves on a boundary. Importantly, this modification does not require to change controllers of the other agents in the system and, under certain conditions, it can make the system string stable. Another advantage is that the output of the controller is feasible (see Fig. 7). A difficulty is that the agent is required to know its own and neighbour's dynamical models. If the neighbour's model is known only approximately, then the wave is not fully absorbed and it partially reflects back. However, the numerical simulations show that the response of the system may still be improved since these schemes are relatively 'robust' to the inaccuracies. This is in agreement with experience from practical implementations, see for instance [20], [9] or [18].

5. Numerical simulations of the soft boundary

The numerical simulations are carried out with *WaveBox*, which is a set of functions and examples in MATLAB that numerically approximates WTFs and BTFs. The *WaveBox* contains a set of examples that show the effect of boundaries and absorbers. Some of the examples are presented in this section. The *WaveBox* was written by the authors and is available at [12].

5.1. Soft boundary performance

In the numerical simulations we use the following OLTFs, which represent a double integrator agent with viscous friction, controlled by a PI controller:

$$M_1(s) = \frac{4s+4}{s^2(s+4)}, \quad M_2(s) = \frac{s+k_p}{s^2(s+3)}. \quad (57)$$

First, consider a path graph of 8 agents with OLTFs $M_{\mathrm{f},i}(s) = M_{\mathrm{r},i}(s) = M_1(s)$ for $i = 1, 2, 3, 4$ and $M_{\mathrm{f},i}(s) = M_{\mathrm{r},i}(s) = M_2(s)$ for $i = 5, 6, 7, 8$ and we set $k_p = 1$. There is a soft boundary located between the 4^{th} and 5^{th} agent. The effect of the soft boundary along with wave-absorbing controllers on the first and rear-end agents is demonstrated in Fig. 5. The reflection at the boundary is revealed by the negative value of the B component.

Since A and B components always sum to to the output, it also validates that our decomposition is correct. Of course, X_i could have been obtained using standard state-space or transfer function approaches, but it would not reveal the local properties (reflections) at the boundary and a way how the signal propagates. This is where our decomposition into waves become useful. Therefore, we think of the wave approach as a complementary tool to the traditional approaches. We have shown in [13] that an absorber implemented on either end shortens the transient in a homogeneous system. In Fig. 6 we evaluate the performance of absorbers in heterogeneous system described above. Comparing the top-left and bottom-left panels, we can see that the soft-boundary absorber does not shorten the settling time if it is not combined with an absorber on either end. For the absorber on the first agent (top-middle panel), the wave keeps reflecting between the soft boundary and the non-absorbing rear-end agent, which prolongs the transient. The implementation of the soft-boundary absorber (bottom-middle panel) shortens the transient a lot. The absorbers implemented on both the first and rear-end agents (top-right panel) cause a change of the steady-state value, as predicted by Lemma 1. This is solved by the soft-boundary absorber (bottom-right panel) or by over-compensating the reference value as we did in [14].

Fig. 7 shows the comparison of the inputs to the fourth agent for (i) the homogeneous system with 8 identical agents (blue solid line) with $M_{\mathrm{f},i}(s) = M_{\mathrm{r},i}(s) = M_1(s)$, (ii) the system with non-identical agents described above without the soft-boundary absorber (green dashed line), and (iii) the system as in (ii) but with the soft-boundary absorber (red pluses). It illustrates the absorber does not change the control effort too much.

5.2. Local effect of the DC gains

A local effect of the BTF DC gains is demonstrated in Fig. 8. It shows the first 140 seconds of the step response of system with $N = 80$. The models are $M_{\mathrm{f},i}(s) = M_{\mathrm{r},i}(s) = M_1(s)$ for $i = 1, \ldots, 40$ and $M_{\mathrm{f},i}(s) = M_{\mathrm{r},i}(s) = M_2(s)$ for $i = 41, \ldots, 80$. The constant k_p is varied. Applying (3)-(9) and (19), we can describe the output of the 41^{st} agent as

$$X_{41}(s) = T_{\mathrm{aa}}(s)A_{40}(s) + (1 + T_{\mathrm{ba}}(s))B_{41}(s), \quad (58)$$

where $B_{41}(s)$ is the wave that first transmitted through the boundary, travelled from the 41^{st} agent to the 80^{th} agent, reflected at the end and then travelled back to the 41^{st} agent,

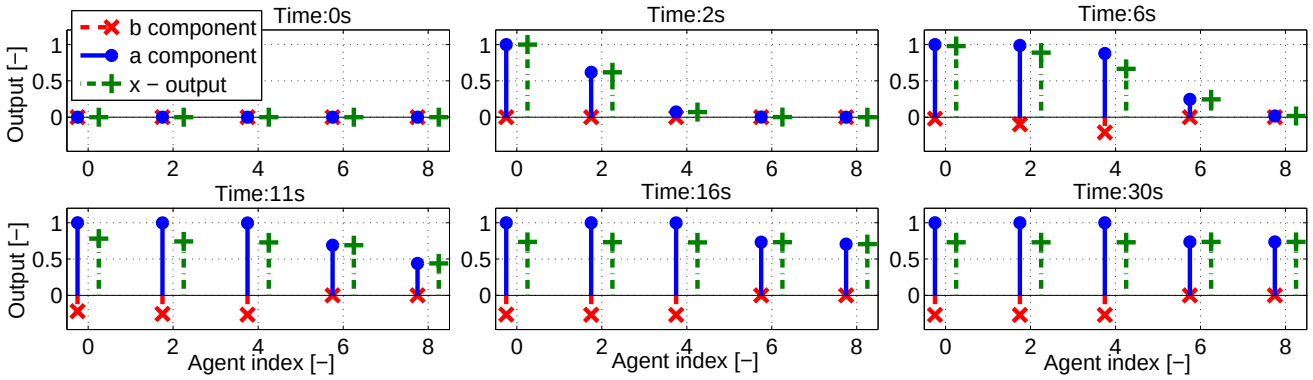

Figure 5: Simulation of the wave propagating in a multi-agent system with the path-graph topology. A response to a step change in X_{ref} is shown. At intermediate times, the wave travels to the soft boundary, where it is transmitted and attenuated by a factor κ_{aa} and reflected by a factor κ_{ab}. As the wave propagates back to the first agent, it forces the first four agents to change their output by κ_{ab} (negative value in this case). The waves are absorbed on 1$^{\mathrm{st}}$ and 8$^{\mathrm{th}}$ agents by the wave-absorbing controllers. The 0$^{\mathrm{th}}$ agent is the input to the system from (10), i.e. $X_0(s) = W_{\mathrm{f},1}(s)$, $A_0(s) = X_{\mathrm{ref}}(s)$ and $B_0(s) = GB_1(s)$.

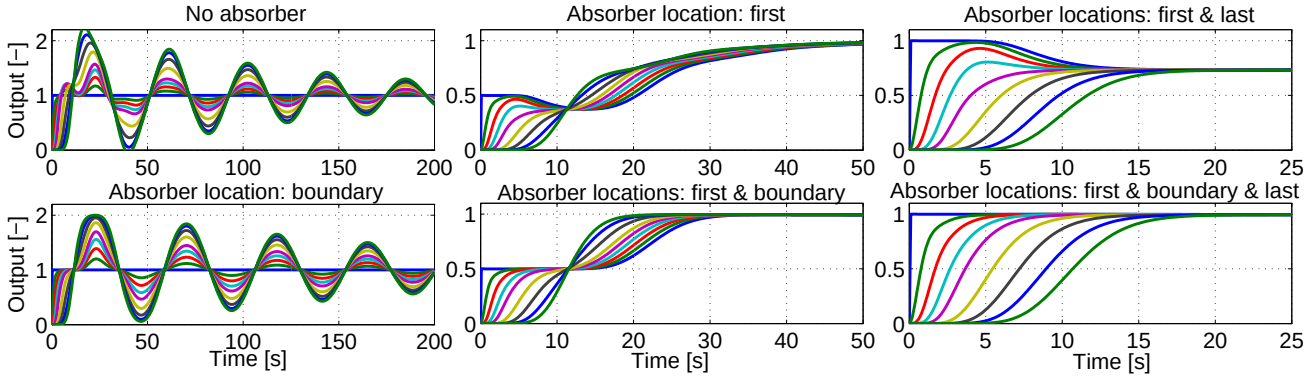

Figure 6: Performance comparison of individual control strategies for a system with soft boundary between agents 4 and 5. $x_{\mathrm{ref}}(t) = 1$.

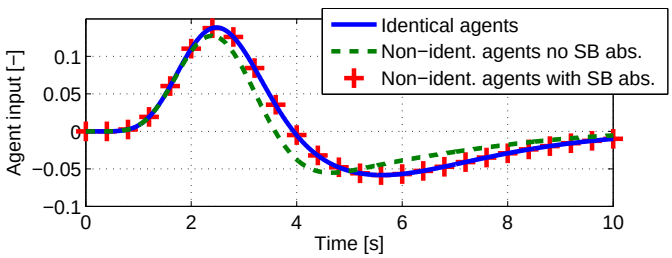

Figure 7: The comparison of the inputs to the fourth agent for three different multi-agent systems. The label 'SB abs.' stands for the soft-boundary absorber.

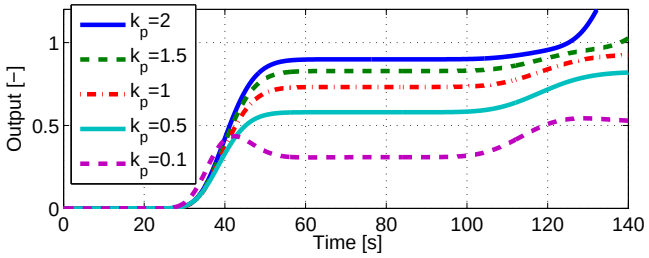

Figure 8: Output of the 41$^{\mathrm{st}}$ agent with $N = 140$ for different values of k_{p}.

hence, $B_{41}(s) = T_{\mathrm{aa}}(s)H^{79}(s)A_{40}(s)$. It takes some time for this reflected wave to propagate, therefore, we can approximate the output $X_{41}(s)$ as $X_{41}(s) \approx T_{\mathrm{aa}}(s)A_{40}(s)$. The approximation is precise in the time-domain until the wave returns back to the 41$^{\mathrm{st}}$ agent ($t \approx 110\,s$). After the initial settling time, the output can be approximated by the DC gain of $T_{\mathrm{aa}}(s)$, because the input is the unit-step in $x_ref(t) = 1$. Hence, $x_{41}(t) \approx \kappa_{\mathrm{aa}}$, $t \in [50, 100]$. The most important feature of the approximation is that it does not consider interactions among other agents. In other words, there can be arbitrary number of agents with various dynamics after the 41$^{\mathrm{st}}$ agent.

6. Conclusion

This paper introduces a wave approach to a multi-agent system with path-graph topology and heterogeneous agents. We define and mathematically describe two basic types of bound-

aries between non-identical agents. Their effect on the waves travelling in the system is captured using transfer functions, which show that part of the wave gets through the boundary and part is reflected back. The travelling waves describe the system from a local point of view.

The wave description allows us to design a feedback controller to compensate the effect of the boundaries, which shortens the settling time. Moreover, such a controller makes the system string stable provided that the system is equipped with at least one wave absorber on the first or rear-end agents.

Appendix A. Proof of Lemma 1

Let us denote $\alpha_\mathrm{r} = 2 + 1/M_{\mathrm{r},\sigma} = 2 + d_1/n_1$ and $\alpha_\mathrm{f} = 2 + 1/M_{\mathrm{f},\sigma+1} = 2 + d_2/n_2$. We will show the DC gain κ_aa of the T_aa transfer function. The derivation of κ_bb is similar.

$$\kappa_\mathrm{aa} = \lim_{s\to 0} T_\mathrm{aa} = \lim_{s\to 0} \frac{H - HG^2}{1 - HG} = \lim_{s\to 0} \frac{1 - G^2}{H^{-1} - G} = \frac{0}{0}, \quad \text{(A.1)}$$

since $\lim_{s\to 0} G = \lim_{s\to 0} H = 1$ for at least one integrator in $M_{\mathrm{r},\sigma}$ and $M_{\mathrm{f},\sigma+1}$. Applying the L'Hopital's rule to (A.1) gives

$$\kappa_\mathrm{aa} = \lim_{s\to 0} \frac{2G}{H^{-2}H'\,(G')^{-1} + 1} = \lim_{s\to 0} \frac{2}{H'\,(G')^{-1} + 1}, \quad \text{(A.2)}$$

where the symbol $'$ denotes the differentiation with respect to variable s. First, the differentiation of (11) yields $G' = \frac{1}{2}\alpha_\mathrm{r}' - \frac{1}{2}\frac{\alpha_\mathrm{r}\alpha_\mathrm{r}'}{\sqrt{\alpha_\mathrm{r}^2-4}}$. For α_r' we get that if $\nu_\mathrm{r} = 1$, then $\lim_{s\to 0}\alpha_\mathrm{r}' < \infty$ and if $\nu_\mathrm{r} > 1$, then $\lim_{s\to 0}\alpha_1' = 0$. The other part of G' is

$$\begin{aligned}\lim_{s\to 0} \frac{\alpha_\mathrm{r}'}{\sqrt{\alpha_\mathrm{r}^2 - 4}} &= \lim_{s\to 0} \frac{d_1' n_1 - d_1 n_1'}{n_1\sqrt{d_1^2 + 4d_1 n_1}} \\ &= \lim_{s\to 0} \frac{\left(s^{(\nu_\mathrm{r}/2)-1}\nu_\mathrm{r} d_{1,0} n_1\right)}{n_1\sqrt{4d_{1,0}n_1}} = \lim_{s\to 0} \nu_\mathrm{r} s^{(\nu_\mathrm{r}/2)-1}\frac{1}{2}\sqrt{\frac{d_{1,0}}{n_{1,0}}}, \quad \text{(A.3)}\end{aligned}$$

where $d_{1,0} = \lim_{s\to 0} s^{-\nu_\mathrm{r}} d_1$ and $n_{1,0} = \lim_{s\to 0} n_1$. Moreover $\lim_{s\to 0}\alpha_\mathrm{r} = 2$. Similarly, $\lim_{s\to 0} H'$ can be evaluated. Then

$$\lim_{s\to 0} \frac{H'}{G'} = \lim_{s\to 0} s^{(\nu_\mathrm{f}-\nu_\mathrm{r})/2}\frac{\nu_\mathrm{f}}{\nu_\mathrm{r}}\sqrt{\frac{n_{1,0}d_{2,0}}{n_{2,0}d_{1,0}}}, \quad \text{(A.4)}$$

where $d_{2,0} = \lim_{s\to 0} s^{-\nu_\mathrm{f}} d_2$ and $n_{2,0} = \lim_{s\to 0} n_2$. Finally, substituting (A.4) into (A.2) yields $\kappa_\mathrm{aa} = \lim_{s\to 0} 2\left(s^{(\nu_\mathrm{f}-\nu_\mathrm{r})/2}\frac{\nu_\mathrm{f}}{\nu_\mathrm{r}}\sqrt{\frac{n_{1,0}d_{2,0}}{n_{2,0}d_{1,0}}} + 1\right)^{-1}$. Assigning the particular values for $\nu_\mathrm{f}, \nu_\mathrm{r}$ gives the result. □

Appendix B. Proof of Lemma 2

The proof is based on [2, Thm. A.2], which states: *A linear system is stable if and only if its transfer function $T(s)$ is analytic in the right-half plane (RHP) and $\|T\|_\infty < \infty$, where $\|T\|_\infty = \sup_{Re(s)>0}|T(s)|$.*

It was proved in [13] that WTF in (6) satisfies $\|G\|_\infty \le 1$. Hence, we show only when WTF is analytic in RHP.

First, we treat the square root function in (6). By [23, pp. 99-100], $f(z) = \sqrt{z}$ is analytic everywhere, except for the non-positive real axis. Therefore, $f_2(\alpha) = \sqrt{\alpha^2 - 4}$ in (6) is analytic for $\alpha \notin [-2, 2]$. Since $\alpha(s) = 2 + 1/M(s)$, $M(s)$ must not be equal to $(-\infty, -1/4]$ for $\Re\{s\} > 0$. We can test this condition by the Nyquist plot of $M(s)$. This follows from the Maximum modulus principle [23, Thm. 4.5] and the assumption that $M(s)$ has no CRHP pole except for ν poles at origin. So $M(j\omega)$ must not not intersect the real interval $(-\infty, -1/4]$ for $\omega \in (0, \infty)$.

The other part of the $G(s)$, $1 + 0.5/M(s)$, is analytic in the CRHP if and only if there are no CRHP zeros of $M(s)$. If both parts of $G(s)$ are analytic, their difference is also analytic and $G(s)$ is a stable transfer function. □

Appendix C. Proof of Theorem 5

Consider a system with one soft boundary (between σ and $\sigma + 1$) with models $M_{\mathrm{f},i} = M_{\mathrm{r},i}$, $M_{\mathrm{f},j} = M_{\mathrm{r},j}$, where $i = 1, ..., \sigma$ and $j = \sigma + 1, ..., N$. The proof for multiple soft or hard boundaries is analogous. We omit the 's' operator from the equations.

First, consider a wave absorber only on the first agent. Then the combination of (4), (5), (48) and (49) gives

$$\frac{X_p}{X_\mathrm{ref}} = \begin{cases} G^p + G^{2\sigma+1-p}H^{2(N-\sigma)} & \text{if } p \le \sigma, \\ G^\sigma H^{p-\sigma} + G^\sigma H^{2N+1-\sigma-p} & \text{if } p > \sigma. \end{cases} \quad \text{(C.1)}$$

In the alternative case of the wave absorbers implemented either on the rear-end agent, or on both the ends, we get

$$\frac{X_p}{X_\mathrm{ref}} = \begin{cases} G^p & \text{if } p \le \sigma, \\ G^\sigma H^{p-\sigma} & \text{if } p > \sigma. \end{cases} \quad \text{(C.2)}$$

Since G and H are asymptotically stable, and $\|G\|_\infty \le 1$ and $\|H\|_\infty \le 1$, then (C.1),(C.2) are asymptotically stable too and their the H_∞ norm is limited regardless of N. By Definition 3, these two systems are also L_2 string stable.

Now, we prove stability for no wave absorber on either ends, but with a soft-boundary absorber. First, we show a way to find the transfer function from X_ref to X_1 for the system with $\sigma = 3$ and $N = 5$. In this case, $A_1 = GX_\mathrm{ref} - G^7H^4A_1$ and $B_1 = G^6H^4X_\mathrm{ref} - G^7H^4B_1$, hence

$$\frac{X_1}{X_\mathrm{ref}} = \frac{A_1 + B_1}{X_\mathrm{ref}} = \frac{G + G^6H^4}{1 + G^7H^4}, \quad \frac{X_2}{X_\mathrm{ref}} = \frac{G^2 + G^5H^4}{1 + G^7H^4}, \quad \text{(C.3)}$$

and so on. For the pth agent, we have

$$\frac{X_p}{X_\mathrm{ref}} = \begin{cases} \dfrac{G^p + G^{2\sigma+1-p}H^{2(N-\sigma)}}{1 + G^{2\sigma+1}H^{2(N-\sigma)}} & \text{if } p \le \sigma, \\ \dfrac{G^\sigma H^{p-\sigma} + G^\sigma H^{2N-\sigma-p+1}}{1 + G^{2\sigma+1}H^{2(N-\sigma)}} & \text{if } p > \sigma. \end{cases} \quad \text{(C.4)}$$

Note that the transfer functions between two arbitrary agents can be expressed similarly.

By (6), $M/(1 + 2M) = G/(1 + G^2)$. If $M/(1 + \lambda M)$ is stable for $\lambda \in (0, 4]$, and if there are neither CRHP poles nor CRHP zeros in $M(s)$, then the Nyquist curve of $M(s)$ does not encircle

the point $[-1/4, 0]$. Hence, $M(s)$ does not intersect $(-\infty, -1/4]$. Thus, if the conditions in Lemma 2 hold, then $M/(1 + 2M)$ is stable and also $G/(1 + G^2)$ is stable. Using $\|G\|_\infty \leq 1$ and $\|H\|_\infty \leq 1$, the transfer function $G/(1 + G^2 G^{q_1} H^{q_2})$ is asymptotically stable for $q_1, q_2 \in \mathbb{N}$. Furthermore, since G and H are stable, then the following transfer function is stable for $q_3, q_4 \in \mathbb{N}$

$$\frac{G G^{q_3} H^{q_4}}{1 + G^2 G^{q_1} H^{q_2}}. \tag{C.5}$$

Comparing (C.5) with (C.4), we proved asymptotic stability for the case with no absorber at the end and boundary control law by Theorem 3. The proof for the control law from Theorem 4 can be carried out analogously. The only difference is in different powers of G and H in (C.1),(C.2) and (C.4). □

References

[1] P. Barooah, P. Mehta, J. Hespanha, Mistuning-Based Control Design to Improve Closed-Loop Stability Margin of Vehicular Platoons, IEEE Trans. Automat. Control 54 (9) (2009) 2100–2113.

[2] R. Curtain, K. Morris, Transfer functions of distributed parameter systems: A tutorial, Automatica 45 (5) (2009) 1101–1116.

[3] T. Dhaene, D. D. Zutter, Selection of lumped element models for coupled lossy transmission lines, IEEE Trans. Comp. Aided Design Integ. Circuits Syst. (July) (1992) 805–815.

[4] S. K. Dwivedy, P. Eberhard, Dynamic analysis of flexible manipulators, a literature review, Mechanism Machine Theory 41 (7) (2006) 749–777.

[5] J. Eyre, D. Yanakiev, I. Kanellakopoulos, A Simplified Framework for String Stability Analysis of Automated Vehicles, Veh. Syst. Dynamics (1998) 375–405.

[6] L. Galbusera, M. P. E. Marciandi, P. Bolzern, G. F. Trecate, Control schemes based on the wave equation for consensus in multi-agent systems with double-integrator dynamics, in: Conf. Decision Control, no. 1, IEEE, 2007.

[7] I. Herman, D. Martinec, Z. Hurák, M. Sebek, Nonzero Bound on Fiedler Eigenvalue Causes Exponential Growth of H-Infinity Norm of Vehicular Platoon, IEEE Trans. Automat. Control 60 (8) (2015) 2248–2253.

[8] S. Knorn, A. Donaire, J. C. Agüero, R. H. Middleton, Passivity-based control for multi-vehicle systems subject to string constraints, Automatica 50 (12) (2014) 3224–3230.

[9] E. Kreuzer, M. Steidl, Controlling torsional vibrations of drill strings via decomposition of traveling waves, Arch. Appl. Mechanics 82 (4) (2011) 515–531.

[10] B. Lesieutre, Impedance matching controllers to extinguish electromechanical waves in power networks, in: IEEE Internat. Conf. Control Appl., 2002.

[11] F. Lin, M. Fardad, M. R. Jovanović, M. R. Jovanovic, Optimal control of vehicular formations with nearest neighbor interactions, IEEE Transactions on Automatic Control 57 (9) (2012) 2203–2218.

[12] D. Martinec, WaveBox (2015).
URL `https://www.mathworks.com/matlabcentral/fileexchange/51958-wavebox`

[13] D. Martinec, I. Herman, Z. Hurák, M. Šebek, Wave-absorbing vehicular platoon controller, Eur. J. Control 20 (2014) 237–248.

[14] D. Martinec, I. Herman, M. Sebek, Two-sided wave-absorbing control of a heterogenous vehicular platoon, in: 19th IFAC World Congress, no. 1986, 2014.

[15] C. Mei, Wave control of vibrations in multi-story planar frame structures based on classical vibration theories, J. Sound Vibration 330 (23) (2011) 5530–5544.

[16] W. J. O'Connor, Wave-Based Analysis and Control of Lump-Modeled Flexible Robots, IEEE Trans. Robotics 23 (2) (2007) 342–352.

[17] W. J. O'Connor, Wave-like modelling of cascaded, lumped, flexible systems with an arbitrarily moving boundary, J. Sound Vibration 330 (13) (2011) 3070–3083.

[18] W. J. O'Connor, F. Ramos de la Flor, D. J. McKeown, V. Feliu, Wave-based control of non-linear flexible mechanical systems, Nonlinear Dynamics 57 (1-2) (2008) 113–123.

[19] R. Olfati-Saber, J. Fax, R. Murray, Consensus and cooperation in networked multi-agent systems, Proc. IEEE (January) (2007) 215–233.

[20] M. Saigo, N. Tanaka, D. H. Nam, Torsional vibration suppression by wave-absorption control with imaginary system, J. Sound Vibration 270 (4-5) (2004) 657–672.

[21] W. Singhose, S. Derezinski, N. Singer, Extra-insensitive input shapers for controlling flexible spacecraft, J. Guidance Control Dynamics 19 (2) (1996) 385–391.

[22] L. Sirota, Y. Halevi, Fractional order control of the two-dimensional wave equation, Automatica 59 (2015) 152–163.

[23] E. M. Stein, R. Shakarchi, Complex Analysis, Princeton lectures in analysis, Princeton University Press, New Jersey, 2010.

[24] D. Swaroop, J. Hedrick, String stability of interconnected systems, IEEE Trans. Automat.c Control 41 (3) (1996) 349–357.

[25] F. Tangerman, J. Veerman, B. Stosic, Asymmetric decentralized flocks, IEEE Trans. Automat. Control 57 (11) (2012) 2844–2853.

[26] K. Yamamoto, M. Smith, Mass chains with passive interconnection: Complex iterative maps and scalability, in: Conf. Decision Control, 2013.